Towards testing of a second-generation bladed receiver

Cite as: AIP Conference Proceedings **2126**, 030044 (2019); https://doi.org/10.1063/1.5117556
Published Online: 26 July 2019

John Pye, Ehsan Abbasi, Maziar Arjomandi, Joe Coventry, Farzin Ghanadi, Graham Hughes, Jin-Soo Kim, Li Ma, Ali Shirazi, Juan F. Torres, Felix Venn, Ye Wang, and Meige Zheng

Towards Testing of a Second-Generation Bladed Receiver

John Pye[1, a)], Ehsan Abbasi[1], Maziar Arjomandi[2], Joe Coventry[1], Farzin Ghanadi[2], Graham Hughes[3], Jin-Soo Kim[4], Li Ma[3], Ali Shirazi[1], Juan F. Torres[1], Felix Venn[1], Ye Wang[1] and Meige Zheng[1]

[1]*Research School of Electrical, Energy and Materials Engineering, The Australian National University, Canberra ACT 0200, Australia*
[2]*Centre for Energy Technology, University of Adelaide, Adelaide SA 5005, Australia*
[3]*Department of Civil and Environmental Engineering, Imperial College, London SW7 2AZ, United Kingdom*
[4]*CSIRO Energy Centre, 10 Murray Dwyer Circuit, Mayfield West NSW 2304, Australia*

[a)]Corresponding author: john.pye@anu.edu.au

Abstract. A bladed receiver design concept is presented which offers a >2% increase in overall receiver efficiency after considering spillage, reflection, emission and convection losses, based on an integrated optical-thermal model, for a design where the working fluid is conventional molten salt operating in the standard 290–565°C temperature range. A novel testing methodology is described, using air and water to test the receiver when molten salt facilities are not available. Technoeconomic analysis shows that the receiver could achieve a 4 AUD/MWhe saving in levelised cost of energy, but only if the bladed receiver design can be implemented at no additional cost.

CONCEPT

Bladed receivers take flat or convex tube panels, as used in state-of-the-art molten salt receivers, and reconfigure those tube panels into bladed or finned structures. This modified arrangement allows increased light-trapping and overall increased receiver efficiency, while continuing to respect the peak-flux limits that apply to receiver tubes. The bladed receiver concept as discussed here was first proposed by Ho et al [1-3], although several similar and very interesting concepts based on rearranged tube panels have also been developed by Vant-Hull et al [4], by Wagner et al [5] and by Puppe et al [6]. A first-generation bladed receiver was tested by Ho et al in 2016 [2].

In the present work, we consider a configuration where flow passes through blades formed from pipework loops as shown in Figure 1. Flow enters the outermost loop and passes around and around towards the back of the loop. Several blades are connected in parallel, with manifolds connecting the inlets and outlets. After the blade outlet manifold, the flow path is divided into several parallel serpentine flow-paths that pass up and down on the 'back wall' behind the blades. Finally, we note that there is a small additional amount of pipework surrounding the blades and back-wall, referred to as the 'edge section', where fluid is pre-heated in several parallel flow paths, before passing to the blade inlet manifold.

The benefits of this receiver configuration are considered to be the following. Firstly, the design allows receivers to handle more highly concentrated solar irradiance at the aperture plane, since the blade surfaces can be oriented to be parallel to the prevailing direction of the incident rays, causing the incident rays to be absorbed over a larger surface area than the case for a convex external surface; essentially the peak flux constraints that apply to convex receivers are eased by 'folding up' a larger surface area into the same aperture space, with similar thinking to that of the SCRAP receiver of Lubkoll et al [7]. Secondly, the resulting blade structures form light-trapping quasi-cavities that greatly decrease reflection losses. Thirdly, the flow path configuration is arranged so that the hottest surfaces will be the back-wall surfaces, whose thermal emissions will be reduced due to the low view factor to the surroundings. Finally, by

SolarPACES 2018
AIP Conf. Proc. 2126, 030044-1–030044-9; https://doi.org/10.1063/1.5117556
Published by AIP Publishing. 978-0-7354-1866-0/$30.00

FIGURE 1. The second-generation bladed receiver concept. Cool fluid is introduced at the tips of the blades and circulates around towards the back. Cavity effects help to reduce losses from the hotter parts of the receiver, and the bladed structure also helps to increase light trapping. Blades are made up of pipe loops to simplify fabrication.

allowing the aperture flux to be increased, the design permits the use of more concentrated aiming strategies, with the potential to allow an overall smaller receiver, with consequently lower convection and thermal emission losses, while still respecting peak flux at the level of individual tubes.

In this paper, we present results of a detailed analysis of a bladed receiver with a molten solar salt working fluid, designed for installation on a polar field system similar to the PS10 plant [8]. The boundary conditions are that molten salt is to be heated from 290°C to 565°C, which is understood to be a temperature range for molten salt which is considered safe for this material in practice [9]. A bladed design is identified which achieves a clear improvement in overall receiver efficiency relative to a best-case flat receiver designed for the same PS10 solar field. Next, a methodology is described for testing a scaled-down receiver based on this large-scale design. A challenging requirement for the testing is that molten salt is not available as a working fluid at the available test facility in CSIRO in Newcastle, Australia. Next, we present the detailed design of the receiver which is currently under construction and will be tested in late 2018. Finally, we give the results of a techno-economic analysis of the bladed receiver design, and show that despite the clear performance benefits it will be challenging to benefit from this design commercially unless it can be fabricated with only minimal increase in cost relative to the flat receiver.

INTEGRATED MODELLING

Steady-state modelling of a bladed receiver adapted to the PS10 solar field [8] was conducted, integrating the heliostat field with slope errors, sun-shape and aiming strategy, the light absorption on the tube banks, radiative emission losses, convection losses, tube thermal resistance, and internal heat transfer to the molten salt working fluid. An identical integrated modelling process was also developed for the design of a flat receiver using the same tower and heliostat field, to be used as a comparison basis.

Optical simulations and radiative view factor calculations have been performed using the *Tracer* code for Monte-Carlo ray tracing (MCRT) [10, 11]. SolarPILOT [12] was used to calculate the aim-points for the heliostat field on the back-wall of the flat and bladed receivers with a constrained maximum tube-plane flux of 1.2 MW/m² for both flat and bladed receivers. In the optical simulations of both bladed and flat receivers, tube panels (coated with Pyromark, surface absorptivity 94.0%) were approximated as flat panels, with an effective absorptivity of 96.1% adjusted to allow for the light-trapping effect of the crevices between receiver tubes. This approximation was tested using higher-accuracy MCRT simulation of the more realistic geometry.

Convection simulations were performed using computational fluid dynamics (Reynolds-averaged Navier Stokes simulations in OpenFOAM), validated against experimental data from smaller-scale wind-tunnel experiments [13, 14]. Although detailed CFD calculations have been completed, for this analysis they were not closely coupled into the integrated model; instead, uniform convection coefficients were applied here. For the flat receiver a value of 16

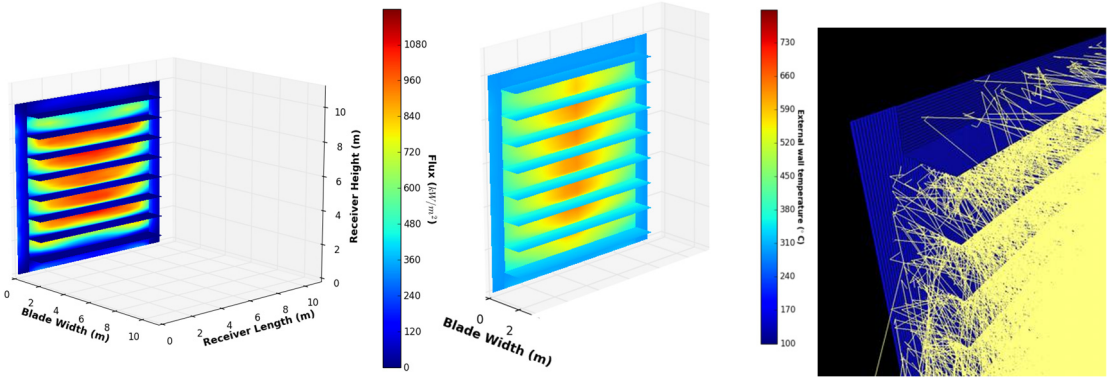

FIGURE 2. Flux (left) and temperature (centre) distributions on a full-scale bladed receiver designed for the PS-10 solar tower (total aperture size 10 m × 10 m, blade lengths 1 m, margin width 0.75 m), based on integrated modelling; Right, details of a ray-tracing study to examine the effective absorptivity assumption used to simplify tube banks into flat panels.

W/m²K. For the bladed receiver, lower per-area convection is expected, and the value of 8 W/m²K was used in the present analysis [13, 15].

Thermal emissions were determined via a surface-to-surface radiosity method, with grey diffuse-surface view factors calculated by MCRT using *Tracer*. In the case of the flat receiver, all view factors were set to one. The effective emissivity of tube banks (approximated as flat surfaces, as for absorptivity) was calculated from the temperature-dependent surface emissivity of aged Pyromark 2500 [16, 17] .

Internal heat transfer was modelled using one-dimensional hydrodynamic models incorporating pressure drops, tube conduction, internal convection coefficients and minor losses, for a realistic pipe-network flow path [17]. Thermophysical properties for molten salt, approximated as incompressible, were used. The salt inlet temperature for both receiver types was 290°C. The integrated model, solving incident flux, internal heat transfer, convection and radiation, was solved by iteratively adjusting the external surface temperatures until next external heat flows matched the next internal heat flows. Finally, in an outer iteration loop, the flow rate was adjusted to give an outlet temperature of 565°C.

To establish an improvement relative to conventional flat/convex receivers, a flat receiver design was modelled based on optimised flux conditions at the focal plane. The optimal receiver design was found with an aperture size of 10 m × 10 m, and with a flowpath made up of 25 panels of 6.7 tubes per panel on average, in a edges-to-centre flow configuration. The inclination angle of the receiver was 16° downward from vertical. The inlet pressure was 14.02 bar and the outlet pressure was 1 bar. The optimal receiver was found to have an efficiency of 91.66%, with losses of 0.74% due to spillage, 3.88% due to reflection, 2.64% due to convection and 1.09% due to thermal emissions.

Next, a range of bladed receiver configurations were assessed and refined. After examining long and short blade configurations, aiming strategies, tilt angles, tube sizes and flow path configurations, a compromise design was identified which achieved a >20% reduction in overall receiver losses at design conditions relative to the optimal flat receiver, based on the model. In this design, the overall receiver aperture was equal to that of the flat receiver (10 m × 10 m), with a 0.75 m wide edge section surrounding an 8.5 m × 8.5 m bladed section with eight blades of length 1 m. The receiver is tilted 36° downward from vertical. The tube size is 50.8 mm OD, with flow topology passing in parallel through the edges, then in parallel through the blades, then in an edges-to-centre flow with tube banks similar to the flat receiver. The overall receiver efficiency was 94.20%, with losses of 0.76% due to spillage, 1.95% due to reflection, 1.97% due to thermal emissions, and 1.12% due to convection. With this level of performance, the bladed receiver design was considered sufficiently interesting to be advanced to the stage of detailed design and testing.

Some key observations arose during the integrated modelling of the full-scale receiver. Firstly, even with aggressive aiming strategies, it is not possible reduce the size of the receiver significantly without increasing spillage losses. The largest spots from the furthest heliostats prevent this from being possible. Hence, a key aspiration of the bladed receiver, which was to facilitate a bladed design without any increase in total tube mass by 'folding up' the tube banks into a smaller aperture [3], proved to be impossible. Secondly, convective losses for long blades become excessive, and it appears that a larger number of short blades will be preferable. Thirdly, a 'edge section' surrounding

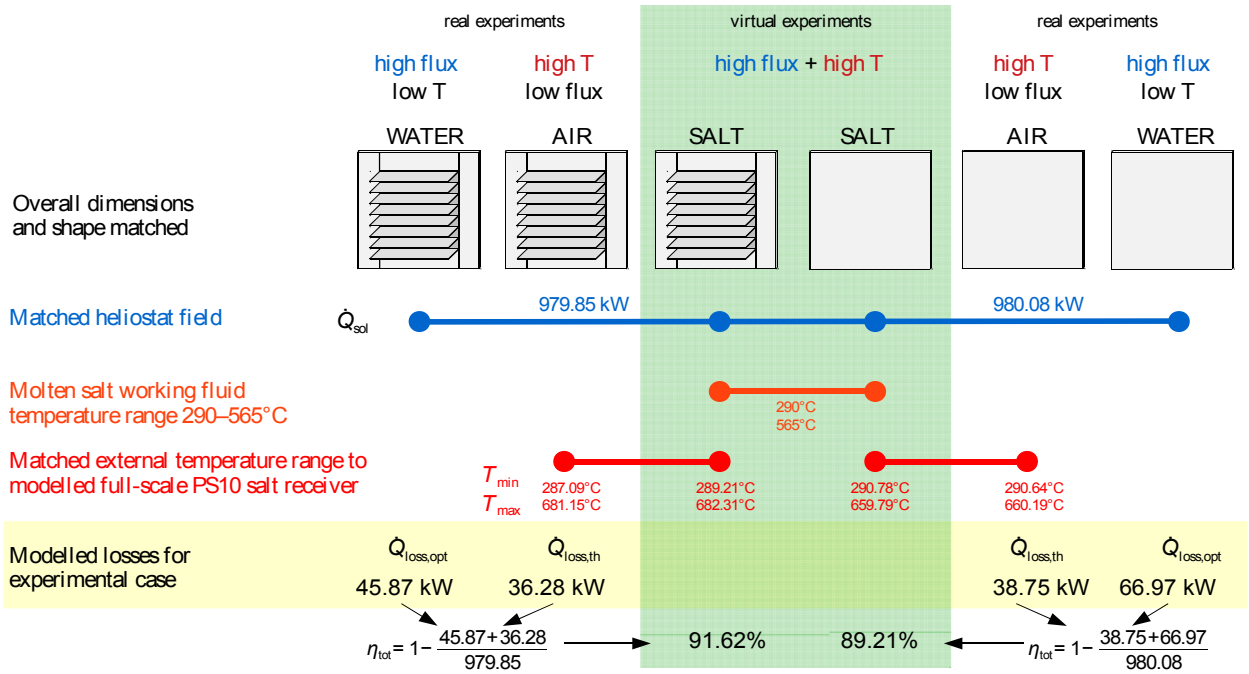

FIGURE 3. Low-flux high-temperature testing with air is combined with high-flux low-temperature testing with water to separately assess the thermal and optical losses of bladed and flat receivers. These results are combined to provide results for a 'virtual experiment' for the performance of a high-flux high-temperature receiver with molten salt, which is necessary since the available test facilities at CSIRO do not currently permit testing with a molten salt working fluid.

the bladed area allows a reduction in total tube mass without increasing spillage losses, in a similar way to the 'pancake' or outer aperture region of the SG4 Big Dish receiver [18].

TESTING METHODOLOGY

Testing is required to validate the above modelling result, and is an activity being conducted currently within the project. The CSIRO solar-thermal test facility in Newcastle, Australia is being used for this on-sun testing.

Ideally, this test would be conducted with a molten salt working fluid, in a receiver that has been faithfully scaled-down from a realistic full-scale design, and in such a way as to realistically demonstrate the improvement in performance which could be expected from the full-scale design. However, a key challenge for the test program was the lack of equipment at CSIRO to allow testing with molten salt.

Starting with the integrated model design of the previous section, designs for two full-scale molten salt receivers were known. The first was an optimised flat receiver, and the second was a bladed design, not optimised, but predicted by the model to perform significantly better than the flat receiver – when both receivers are assumed to be mounted at the same location on an identical solar field, and illuminated by identical heliostats. The two receivers need not be installed with the same size or inclination angle, but the heliostat field was at least assumed to be immutable.

In order to test the conclusions from the integrated modelling, and noting that molten salt was not available, a series of experiments (Figure 3) had to be planned using air and water as the working fluids so as to reproduce, firstly, the external temperature distribution for the purpose of determining thermal performance and, secondly, the incident flux distribution for the purpose of determining optical performance.

In the case of air tests, only a small numbers of heliostats will be used, for a low-flux high-temperature experiment. Compressed air at 7 bar (absolute) is pre-heated and enters the receiver. The heating and flow rates are adjusted to ensure that the minimum and maximum external surface temperatures match those of the full-scale molten salt receiver. Since the incident heat fluxes are low, the reflective losses in this case are nearly negligible. The known direct normal irradiance and instantaneous field optical efficiency can be used to estimate the total energy input. Calorimetry on the air passing through the receiver completes the picture, and allows the thermal losses from this receiver to be estimated. For the air testing, it was important to match the distribution of external wall temperatures

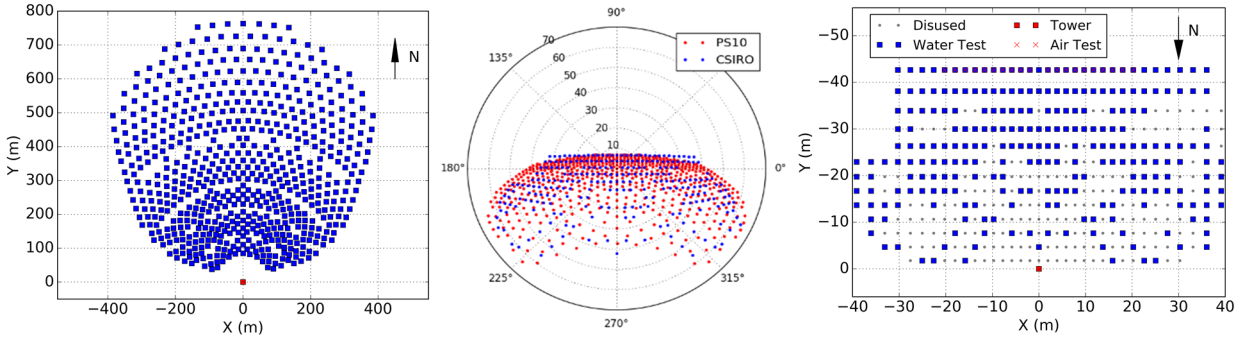

FIGURE 4. Selection of heliostats for on-sun testing, in order to obtain a good match between the angular distribution of incident flux on the bladed receiver. Left, the PS10 field layout. Right, the CSIRO heliostat layout. Centre, the angular positions of heliostats for both fields as seen from the receiver, when looking towards the geometric centre of each field.

as closely as possible. For this reason, a group of far-off heliostats was chosen so that as much radiation as possible would hit the backwall of the bladed receiver. The impact of different choices was evaluated using the integrated model, which was adapted to solve air and water flows in a reduced-scale design. Also, for the air testing, the convective effects should be as close as possible to those of the full-scale receiver. Hence, the receiver tilt angle was matched to that selected for the full-scale receiver.

In the case of water tests, a large number of heliostats will be used, for a high-flux low-temperature experiment. Cold water will be introduced at mains water pressure, and circulated at a high flow rate through the receiver such that its exit temperature is well below its boiling temperature. In this mode, the thermal losses are nearly negligible, and calorimetry together with the direct normal irradiance and field optical efficiency can be used to estimate the optical efficiency of the receiver. For the water testing, it was important to match the optical effects as closely as possible (Figure 4). For this reason, the down-tilt angle of the receiver was increased such that the incident angular distribution of rays on the small-scale bladed receiver matched as closely as possible that experienced by the full-scale design. It is noted that the tower height to heliostat distance ratio is much greater for the CSIRO tower system compared to the PS10 system.

In order to determine the number of heliostats that could be used for the high-flux water test, the outlet pressure capacity of the available water pump was a constraint. The largest possible number of heliostats is needed for the water tests, since integrated modelling shows that the bladed receiver only achieves benefits relative to the flat receiver when the incident flux is sufficiently high, above a threshold. Benefits relative to a flat receiver were calculated to require at least approximately 100 heliostats from the CSIRO tower. This is because the combined thermal losses from a bladed receiver, especially if the backwall size is equal, are somewhat higher than the combined thermal losses from a flat receiver (the emission losses for bladed are slightly lower after considering view factor and temperature distribution effects, while the convective losses are higher due to a similar convection coefficients but significantly increased exposed surface area). Meanwhile, the optical losses from the bladed receiver are lower as a fraction of the incident energy. If the incident energy flux is high, then the optical savings exceed the thermal losses. It was necessary to at least try to choose an experimental flux level that was high enough for us to see the conditions where a bladed configuration shows an overall benefit, as is does for the full-scale bladed receiver case with our modelled PS10 heliostat field.

The results from the air and water tests can then be superimposed to give an estimate for the efficiency of a molten salt receiver of equal size, for the 'virtual experiment' case of high flux and high temperature, which could not have been tested with either air or water on their own. Modelling of all of these cases suggest that experimental observations will show a performance improvement in the on-sun 'virtual experiment' that is consistent with the results obtained for the full-scale model. An uncertainty analysis will be used [19] to ascertain whether an experimental performance improvement can be claimed to be statistically significant, or not.

Once a testing methodology was established, the various constraints of air and water testing needed to be carefully evaluated, and a detailed design for the receiver test modules was developed.

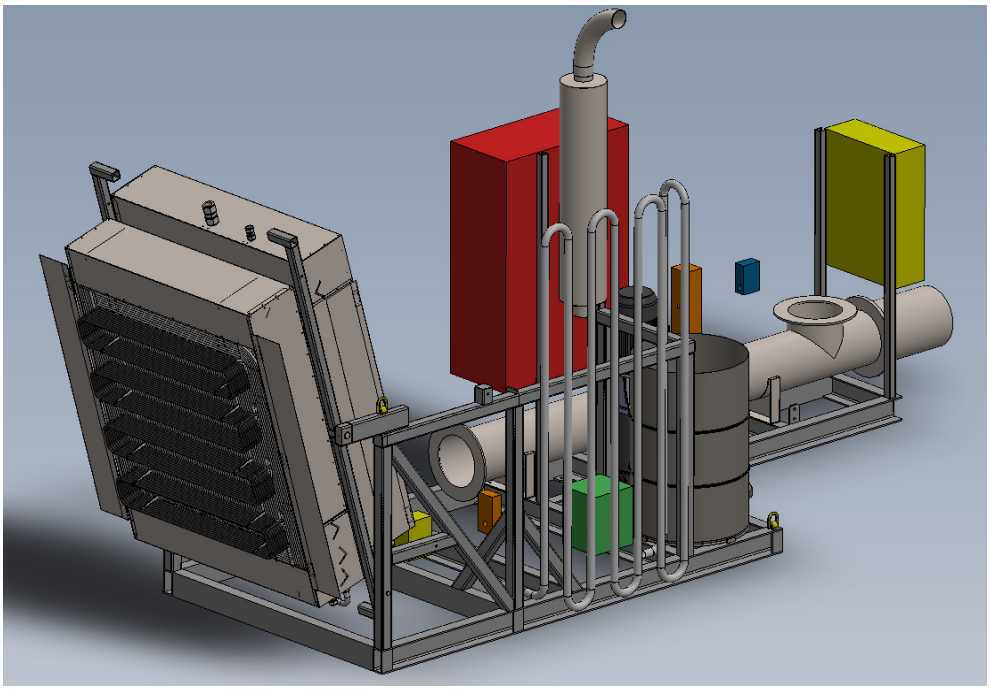

FIGURE 5. Detailed design of a reduced-scale water/air receiver to be tested at CSIRO in September 2018.

DETAILED DESIGN

During detailed design, it was decided that the best approximation to the bladed structure modelled above could be built using tubes coiled around and around into pairs of blades, as shown earlier in Figure 1, although unfortunately so far the optical and thermal effects of the sides of the loops, whether beneficial or detrimental, have not yet been incorporated into the modelling.

The detailed design phase of the project has involved the following essential activities. Tubes have been sized to comply with the Australian Standard for pressure vessels, AS1210-2010, and headers, the tube pitch, and the header-tube welds designed to comply with AS1210-2010. Tube thermal expansion including differential thermal expansion between tubes have been analysed and necessary spacing included. Special 'aligator' tube supports were designed to hold the tubes while minimising shading and facilitating thermal expansion movement. Positioning of supports was decided considering wind and gravity loading. Tube bends were designed considering tooling/machine limitations and ease of fabrication. Four distinct pipework configurations were designed for the required tests, to allow for ready switching between water and air tests of bladed and flat receivers. Tubes were designed for allowable pressure drops and peak fluid velocities. The balance of system components were designed or selected, including a heater, radiator, pump, mixing tank, silencer, valves, several flow meters, pressure and temperature instrumentation, system control, and a test system interface. Fluid drainage, blade tip temperature analysis and blade tip coatings were also considered. The test system currently in fabrication is shown in Figure 5.

TECHNO-ECONOMIC ANALYSIS

A techno-economic analysis was conducted to determine if the bladed receiver might warrant commercial development. Only a crude analysis could be performed, as a detailed design of the full-scale receiver was out of scope for the project. Instead, an analysis was conducted based on cost data from Abengoa [20] for a 910 MWth molten salt external cylindrical receiver with Inconel 625 tubes.

Based on an analysis of the change in mass of the receiver tubes, and a very rough estimate of the likely cost increases in other parts of the system such as the values and controls, tube support structures, and so on, it was

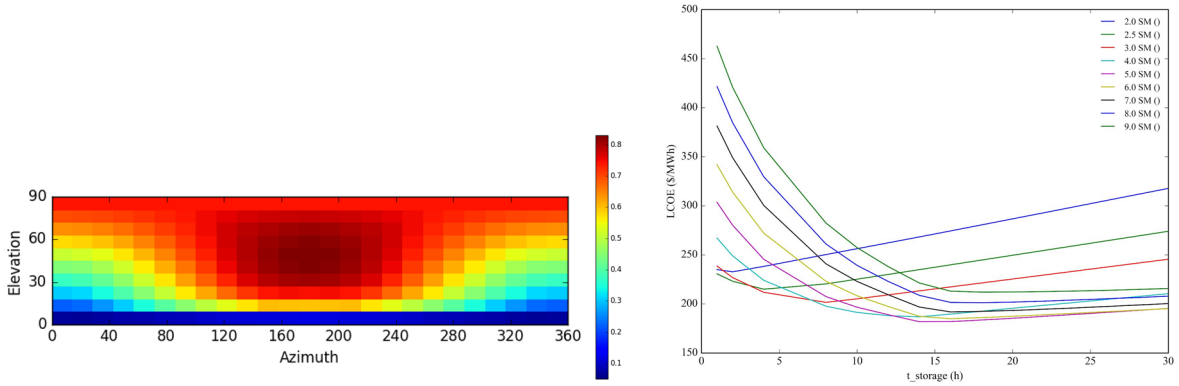

FIGURE 6. Optimisation of the bladed salt receiver system configuration. Left, the optical efficiency lookup table for the PS10 field with the bladed receiver. Right, a parameter study of storage hours and solar multiple to optimise levelised cost of energy.

estimated that the total receiver assembly cost for the bladed design would increase by 18-27%. This was despite the cost of receiver tubes and headers being only approximately 7% of the cost of the original (flat) receiver design.

These costs were incorporated into a generic system model [21] for the PS10 system using SolarTherm [22] and solved using OpenModelica. A collector (field plus receiver) optical efficiency lookup table was calculated using Tracer for a grid of sun positions, for both bladed (Figure 6) and flat receiver designs. The location chosen for the purposes of weather data was Alice Springs in central Australia. The off-design performance of the receiver was determined by running the integrated receiver model at reduced direct normal irradiance values, then fitting a polynomial. Costs for all components other than the receiver (heliostats, storage, power block, land, etc) as well as financial assumptions (discount rate, system life, construction time) were taken to be the default values SAM Version 2017.9.5. The system design was optimised by varying the storage hours and solar multiple (Figure 6).

The result of the techno-economic analysis was that the bladed receiver, if the overall cost increase is 18–27%, provides almost no benefit in reducing the levelised cost of electricity. If the cost of the receiver were the same as the flat receiver, then the LCOE savings would be of the order 4 AUD/MWhe.

These results are not encouraging! However, at least the following few points can be noted: (1) it may be possible to use lower-grade materials for some parts of the bladed receiver, since not all tubes are subject to extreme fluxes; (2) the bladed design has not yet been optimised; the design presented here was found to meet the original performance targets, but greater performance gains might still be possible – for example by increasing the size of the 'edge' region and reducing the size of the bladed region, and using a more peaky aim-point strategy; (3) bladed receivers may provide greater benefits when used in higher-temperature receiver types; (4) there has been no attempt yet to specifically optimise the field layout for this particular receiver type; (5) configurations of bladed receivers adapted to surround receivers have not yet been considered, and may provide other cost reduction opportunities; (6) the design process here was always seeking to maximise efficiency only, whereas a new process could be conducted aiming to reduce LCOE from the start. There are various design configurations that can be considered then, as next iterations, providing that in future work the strong influence of potentially higher costs for new designs are carefully monitored at the same time. It can be noted that the DLR analysis of a similar 'star' design showed a very favourable result in fully optimised configuration, which in that case was obtained by reducing the total material costs as a result of the use of a double-sided tube configuration, rather than through efficiency improvements [6].

CONCLUSIONS

A small but significant gain in receiver efficiency of >2% from bladed receivers was identified after a rigorous integrated modelling study in which a flat receiver design was first optimised for a modelled PS10 heliostat field, with an assumed working fluid of molten salt in all cases, and used as the comparison basis.

Testing for the receiver is aimed at demonstrating experimentally that this bladed receiver can out-perform a properly optimised flat receiver. This has been challenging, as test facilities for a molten salt working fluid were not available at CSIRO. A combination of low-flux high-temperature air testing and high-flux low-temperature water testing was devised to allow the thermal and optical losses to be separately measured. The results can be combined to

give predicted results from a molten salt 'virtual experiment'. Modelling suggests that these experiments will show a performance gain similar to that modelled for the full PS10-scale bladed receiver.

Detailed design has been completed and the final test receiver, capable of operating under the low-flux air and high-flux water cases, is now under construction (as of Aug 2018). The final receiver design makes use of blade 'loops' in order to reduce the amount of supporting structure and simplify the flow-pathing. However, this increases the distance which flow must travel and decreases the number of available parallel flow paths in the bladed section of the receiver. Pressure drop analysis shows relatively high pressure drops are required for this configuration during testing, although large-scale designs with molten salt will not suffer pressure drops to the same extent. Maximum air velocities are high but well below compressible flow limits.

Techno-economic analysis of the bladed receiver concept shows that the efficiency gains could allow savings in the LCOE of up to 4 AUD/MWhe. However, this saving appears to be completely lost once likely cost increases for the bladed receiver are considered, relative to the costs of a flat receiver. This result was obtained for an unoptimised design, however, and several opportunities for further gains were identified, including potentially use in higher temperature receivers, where the performance benefits of this design will be greater.

ACKNOWLEDGEMENTS

The authors gratefully acknowledge the support of the Australian Renewable Energy Agency, 2014/RND010.

REFERENCES

1. C. K. Ho, J. M. Christian and J. D. Pye (2014). "Bladed solar thermal receivers for concentrating solar power", United States Provisional Patent No. 14/535,100 (filed 8 November 2013).
2. C. K. Ho, J. D. Ortega, J. M. Christian, J. E. Yellowhair, D. Ray, J. Kelton, G. Peacock, C. Andraka and S. Shinde (2016). "Fractal-Like Materials Design with Optimized Radiative Properties for High-Efficiency Solar Energy Conversion", Tech. report SAND2016-9526, Sandia National Laboratories.
3. J. Pye, J. Coventry, C. Ho, J. Yellowhair, I. Nock, Y. Wang, E. Abbasi, J. Christian, J. Ortega and G. Hughes (2017). "Optical and thermal performance of bladed receivers". In *SolarPACES 2016 (AIP Conference Proceedings)*, Santiago de Chile.
4. L. L. Vant-Hull, C. R. Applebaugh, J. P. Colaco, C. Easton, S. Gronich, R. W. Hallet, A. Hildebrandt, F. Lipps, R. McFee, J. Raetz and W. Rigdon (1974). "Solar Thermal Power Systems based on Optical Transmission (A Feasibility Study)", Semi-annual progress report to the US National Science Foundation NSF/RANN/SE/GI-39456/PR/73/4, University of Houston and McDonnell Douglas Astronautics West, Houston, Texas.
5. M. Wagner, Z. Ma, J. Martinek, T. Neises and C. Turchi (2014). "Systems and methods for direct thermal receivers using near blackbody configurations", United States Provisional Patent No. 61/993,671 (filed 15 May 2014).
6. M. Puppe, S. Giuliano, C. Frantz, R. Uhlig, R. Flesch, R. Schumacher, W. Ibraheem, S. Schmalz, B. Waldmann, C. Guder, D. Peter, C. Schwager, C. T. Boura, S. Alexopoulos, M. Spiegel, J. Wortmann, M. Hinrichs, M. Engelhardt, M. Aust and H. Hattendorf (2017). "Techno-Economic Optimization of Molten Salt Solar Tower Plants". In *SolarPACES 2017*, Santiago de Chile.
7. M. Lubkoll, T. von Backström, T. Harms and D. Kröger (2015). "Initial Analysis on the Novel Spiky Central Receiver Air Pre-heater (SCRAP) Pressurized Air Receiver". In *SolarPACES 2014 (Energy Procedia)*, Beijing.
8. R. Osuna, R. Olavarrıa, R. Morillo, M. Sánchez, F. Cantero, V. Fernández-Quero, P. Robles, T. López, A. Esteban, F. Céron, J. Talegón, M. Romero, F. Téllez, M.-J. Marcos, D. Martínez, A. Valverde, R. Monterreal, R. Pitz-Paal, G. Brakmann, V. Ruiz and M. S. aPietro Menna i (2006). "PS10, Construction of a 11MW solar thermal tower plant in Seville, Spain". In *Solar-PACES 2006*.
9. J. E. Pacheco (2002). "Final Test and Evaluation Results from the Solar Two Project", Technical report SAND2002-0120, Sandia National Laboratories, Albuquerque, New Mexico.
10. Y. Wang, C.-A. Asselineau, J. Coventry and J. Pye (2016). "Optical performance of bladed receivers for CSP systems". In *Proceedings of the ASME 2016 Power and Energy Conference*, Charlotte, North Carolina.
11. Y. Wang, J. Coventry and J. Pye (2018). "Optical and Radiation Considerations in Bladed Receiver Designs for Central Tower Systems". In *SolarPACES 2018 (accepted oral)*, Casablanca.
12. M. J. Wagner and T. Wendelin (2018). *Sol. Energy* **171**, 185-196.

13. J. F. Torres, F. Ganadi, M. Arjomandi and J. Pye (2018). "Convective Heat Loss from a Bladed Solar Receiver". In *SolarPACES 2018 (accepted oral)*, Casablanca.
14. J. F. Torres, F. Ghanadi, I. Nock, M. Arjomandi and J. Pye (2018). *Int. J. Heat Mass Transfer* **119**, 418-432.
15. I. Nock, W. Logie, J. Coventry and J. Pye (2016). "A Computational Evaluation of Convective Losses from Bladed Solar Thermal Receivers". In *Proceedings of the Asia-Pacific Solar Research Conference*, Canberra.
16. C. K. Ho, A. R. Mahoney, A. Ambrosini, M. Bencomo, A. Hall and T. N. Lambert (2013). *J. Sol. Energy Eng.* **136**, 014502.
17. J. Pye, M. Zheng, J. Zapata, C.-A. Asselineau and J. Coventry (2014). "An exergy analysis of tubular solar-thermal receivers with different working fluids". In *Proceedings of SolarPACES 2014*, Beijing.
18. J. Pye, G. Hughes, E. Abbasi-Shavazi, C.-A. Asselineau, G. Burgess, J. Coventry, W. Logie, F. Venn and J. Zapata (2015). "Development of a Higher-Efficiency Tubular Cavity Receiver for Direct Steam Generation on a Dish Concentrator". In *SolarPACES 2015*, Cape Town.
19. J. Pye, J. Coventry, F. Venn, J. Zapata, E. Abbasi, C.-A. Asselineau, G. Burgess, G. Hughes and W. Logie (2016). "Experimental Testing of a High-Flux Cavity Receiver". In *Proceedings of SolarPACES 2016*.
20. B. Kelly (2010). "Advanced Thermal Storage for Central Receivers with Supercritical Coolants", Tech. Report DE-FG36-08GO18149, Abengoa Solar.
21. M. Wagner and G. Zhu (2011). "A Generic CSP Performance Model for NREL's System Advisor Model". In *SolarPACES 2011*, Granada, Spain.
22. P. Scott, A. de la Calle Alonso, J. T. Hinkley and J. Pye (2016). "SolarTherm: A flexible Modelica-based simulator for CSP systems". In *SolarPACES 2016 (AIP Conference Proceedings)*, Abu Dhabi.